Spectrochimica Acta Part B 144 (2018) 29–37

Contents lists available at ScienceDirect

Spectrochimica Acta Part B

journal homepage: www.elsevier.com/locate/sab

Extracting chemical information from high-resolution Kβ X-ray emission spectroscopy

S. Limandri [1], J. Robledo, G. Tirao *

IFEG-CONICET, Facultad de Matemática, Astronomía, Física y Computación, Universidad Nacional de Córdoba, Ciudad Universitaria, 5000 Córdoba, Argentina

ARTICLE INFO

Article history:
Received 12 December 2017
Received in revised form 5 March 2018
Accepted 12 March 2018
Available online 15 March 2018

Keywords:
High-resolution X-ray emission spectroscopy
Chemical speciation
Principal component analysis
Statistical analysis
Fundamental parameters

ABSTRACT

High-resolution X-ray emission spectroscopy allows studying the chemical environment of a wide variety of materials. Chemical information can be obtained by fitting the X-ray spectra and observing the behavior of some spectral features. Spectral changes can also be quantified by means of statistical parameters calculated by considering the spectrum as a probability distribution. Another possibility is to perform statistical multivariate analysis, such as principal component analysis. In this work the performance of these procedures for extracting chemical information in X-ray emission spectroscopy spectra for mixtures of Mn^{2+} and Mn^{4+} oxides are studied. A detail analysis of the parameters obtained, as well as the associated uncertainties is shown. The methodologies are also applied for Mn oxidation state characterization of double perovskite oxides $Ba_{1+x}La_{1-x}MnSbO_6$ (with $0 \le x \le 0.7$). The results show that statistical parameters and multivariate analysis are the most suitable for the analysis of this kind of spectra.

1. Introduction

Characterizing the oxidation state and the electronic configuration is a challenge typically found when studying and developing new complex materials since magnetic and electrical properties are strongly related to the local electronic structure [1]. Electronic transitions involving molecular orbitals and core-levels are suitable candidates to be chemically sensitive since the character of the molecular orbitals depends on the specific chemical species [2]. Inner-shell X-ray absorption and emission spectroscopies are element-specific techniques that allow to probe changes in the electronic structure and coordination of a selected atom. In contrast to X-ray Absorption Spectroscopy (XAS), X-ray Emission Spectroscopy (XES) studies the filled electron orbitals through the emitted spectra, since it results from the filling of an inner-shell vacancy by an outer shell electron. Both techniques provides complementary information, they are directly related to each other and provide common as well as complementary information on the local structure [3]. Kβ XES is a very powerful technique to study the metal oxidation state compared with K edge XAS since it provides more sensitive and reliable information about the electronic structure, with less dependence on the atomic structure [4].

High-resolution XES (HR-XES) experiments have been widely used for studying the chemical environment and the electronic structure of a wide variety of materials [2–11]. This information can be obtained by measuring changes in some spectral features, such as energy shifts, possible satellite lines, line shapes and relative intensities. For 3*d* transition elements, the high-resolution Kβ spectrum shows a clear sensitivity to the chemical environment [7–11].

Observable changes in the XES spectra can be quantified by many parameters. A spectrum deconvolution can be performed if theoretical calculations are available and if the characteristics of the instrument used in the measurement are known. The spectrum fitting methodology is called the *fundamental parameters method*. Spectral changes can also be quantified by a *statistical procedure*, treating the spectrum as a probability distribution and determining statistical parameters, such as the moments of the distribution. Besides, in samples formed from a simple mixture of compounds with different chemical environment for a certain atom, the fluorescence spectrum emitted by this atom can be considered as a linear combination of the spectra emitted by each compound separately. Therefore, it is possible to find the best linear combination by means of the *minimum squares method*. Another approach, *principal component analysis*, is the application of multivariate analysis to relate the variability in-between spectra from samples with the chemical environment.

In this work, the three methodologies mentioned above are applied to determine the nominal oxidation state of Mn from XES spectra. The strength and weakness of each method, as well as the uncertainties related to them, are discussed in detail. The analyzed samples are divided into two groups: (1) mixtures of Mn^{2+} and Mn^{4+} oxides, (2) double perovskite oxides $Ba_{1+x}La_{1-x}MnSbO_6$ (with $0 \le x \le 0.7$). The analysis performed on the first group was used to study the potentialities and

* Corresponding author.
E-mail address: gtirao@famaf.unc.edu.ar (G. Tirao).
[1] Present address: European Synchrotron Radiation Facility 71, avenue des Martyrs, CS 40220, 38,043 Grenoble Cedex 9, France.

https://doi.org/10.1016/j.sab.2018.03.004
0584-8547/

weaknesses of each method, and to establish a strategy for treating more complicated samples. These strategies were then applied to the second group of samples in order to determine the Mn^{2+}/Mn^{3+} ratio with a reliable error in its estimation. The results show the capability of XES experiments for chemical environment characterization, in a complementary way to other well-established techniques, such as XAS or X-ray and neutron diffraction.

2. Theoretical framework

In transition metal compounds, Kβ X-ray emission spectrum results from fluorescence emissions as a consequence of electronic transitions from 3*p* to 1 *s* levels. The main Kβ region, spread over a ~15 eV interval around the main peak, is split into multiplets, mainly composed of the strong $K\beta_{1,3}$ line and the less intense Kβ′ and $K\beta_x$ satellite structures at lower energies (Fig. 1). This region can provide information about oxidation state, ligand type, and metal-ligand bonding length [2,8–10]. The underlying structures may be explained by the ligand field multiplet model, for which the Kβ′ line is attributed to 3*p*-3*d* exchange interaction, and the $K\beta_x$ line is related to a spin flip of one 3*d* electron [11]. Besides a radiative decay, the relaxation of the ionized atom might occur through a Radiative Auger Effect (RAE) transition [12,13]. In this process, the emitted X-ray photon shares its energy with the ejected electron. Therefore, it has an energy lower than the expected diagram line. The RAE $KM_{2,3}M_{4,5}$ transitions correspond to $K\text{-}M_{2,3}$ transitions (associated with the $K\beta_{1,3}$ line) with the emission of an $M_{4,5}$ electron [14]. This structure is observed as a tail of the main $K\beta_{1,3}$ peak (see Fig. 1) and its intensity varies with the oxidation state for 3*d* transition metals.

Two other structures appear towards the high-energy side of the main $K\beta_{1,3}$ line: the Kβ″ and $K\beta_5$ lines that can be interpreted by the molecular orbital (MO) theory [15]. The Kβ″ line is originated from a transition of an electron in a MO mainly composed by ligand-2*s* states to the 1*s* atomic orbital of the central atom [16,17]. On the other hand, the $K\beta_5$ band which originate mainly in transitions from the $6t_2$ and $5t_{1u}$ MOs, are mostly formed by ligand-2p in the two symmetries, T_d (tetrahedral) and O_h (octahedral), respectively. In addition, for T_d symmetry, there is also a quadrupole contribution due to the atomic contribution of metal-3*d* [17].

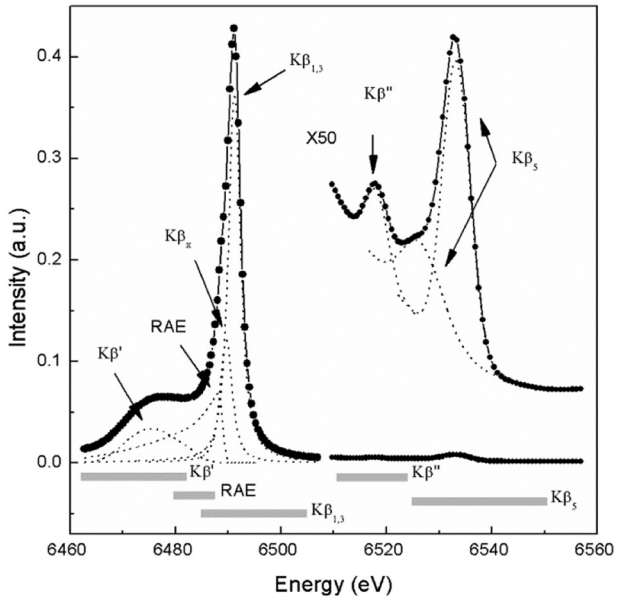

Fig. 1. High-resolution Kβ spectrum of MnO_2. Experimental data (dots). Fitting curve (solid lines) and the corresponding contributions of individual fitting functions (dotted lines). The horizontal grey bars show the energy intervals corresponding to regions where the statistical parameters were calculated.

3. Experimental section

3.1. Sample preparation

3.1.1. Mn oxides mixtures

Different amounts of Mn^{2+} and Mn^{4+} fine polycrystalline oxides powders of high purity (Strem Chemicals Inc.), were mixed to form 12 samples. The resulting molecular concentrations of MnO and MnO_2 oxides were calculated from the mass concentrations measured in the preparation. The name and MnO molecular concentration of each sample are listed below: MnO = 1, $MnO_{0.98}$ = 0.982 (4), $MnO_{0.95}$ = 0.958 (4), $MnO_{0.90}$ = 0.918(4), $MnO_{0.70}$ = 0.741(3), $MnO_{0.50}$ = 0.550(3), $MnO_{0.30}$ = 0.344(2), $MnO_{0.10}$ = 0.122(2), $MnO_{0.05}$ = 0.061(2), $MnO_{0.02}$ = 0.026(2), $MnO_{0.01}$ = 0.014(2), MnO_2 = 0. The MnO_2 molecular concentration can be easily obtained from the MnO molecular concentration. The error in the molecular concentration (number between parentheses) was calculated considering the error of each weighing, and corresponding to the last digit.

3.1.2. Perovskites

Double perovskite oxides (DPOs) with $A_2BB'O_6$ structure are a three-dimensional arrangement of corner-sharing BO_6 octahedral, with the A-type cations, usually alkaline-earth or rare-earth cations, occupying the high coordination sites. The B and B′ ions are different transition metal cations that can be ordered with a doubling of the normal unit cell. This ordering mostly depends on the size and charge difference among cations. The number of *d* electrons and/or the size of the B-site cations may contribute to structural distortions, affecting their magneto-transport properties [18]. B-site ordered DPOs $Ba_{1+x}La_{1-x}MnSbO_6$ (with x = 0, 0.1, 0.2, 0.3, 0.4, 0.5, 0.6, and 0.7) containing Mn^{2+}/Mn^{3+} and Sb^{5+} as B and B′ ions respectively, were studied. These DPOs were specifically developed for technological purposes [7]. As Ba^{2+} content increases, it is expected that Mn^{2+} oxidizes to Mn^{3+} decreasing the difference of charge between B and B′. The nominal Mn oxidation state for these samples is $+2(1+x)$. The DPOs were synthesized as polycrystalline powders by traditional ceramic methods in air [7]. Commercial manganese oxides MnO, Mn_2O_3, MnO_2 were used as standards [19].

3.2. XES measurements

Kβ HR-XES spectra were measured using a Johann-type single crystal spectrometer based on a spherically focusing Si crystal analyzer operated at nearly back-diffraction geometry, in 1:1 Rowland geometry [16]. The diameter of the Rowland circle (410 ± 2) mm corresponds to the curvature radius of the crystal analyzer. The whole spectrometer (sample holder, analyzer and detector) is enclosed in an evacuated chamber. The spectrum of a cobalt-target X-ray conventional tube, operated at 40 mA and 37 kV, was used as irradiation source. Kβ emission spectra were recorded by scanning the energy range [6462–6557] eV in steps of about 0.4 eV around the $K\beta_{1,3}$ main line. The Bragg angle corresponding to the Mn-$K\beta_{1,3}$ line is 84.21° for the (440) reflection of the Si (110) crystal analyzer used, thus obtaining an energy resolution of about 2 eV for this line (for calculation details see Ref. [20]). With a spot size of 2.5 mm^2 the measured counting rate at the $K\beta_{1,3}$ line for $Ba_{1.4}La_{0.6}MnSbO_6$ and MnO was around 80 cps and 1000 cps, respectively. Signal-to-background ratio was better than 70, in both cases.

4. Parameters studied

4.1. Fundamental parameters method

For the implementation of this method in the main $K\beta_{1,3}$ region four structures were used for representing the contribution of the lines Kβ′, RAE, $K\beta_x$ and $K\beta_{1,3}$. Fig. 1 shows for example, the fitting for the MnO_2 spectrum using a Gaussian function for the Kβ′ structure, and two Voigt functions to represent the $K\beta_x$ and $K\beta_{1,3}$ peaks (Gaussian widths

are equal to the experimental resolution). A Gaussian profile was used for the Kβ′ structure because it can be considered as a band [11] and Voigt profiles were used for the $K\beta_x$ and $K\beta_{1,3}$ lines since they are almost single transitions. Additionally, because of its asymmetric shape, an Exponentially Modified Gaussian (EMG) function was used to account for the RAE process [12]. To fit the experimental spectrum in the high-energy region, it was important to remove the background, which comes from the contribution of the tail towards the high energy side of the main $K\beta_{1,3}$ line [21]. This was done by using a Lorentzian function. Afterwards, 1(2) and 2(3) Voigt functions were used for describing, respectively, the Kβ″ and $K\beta_5$ lines in spectra with MnO molecular concentration lower (higher) than 30%.

All these structures may be affected by the Mn oxidation state. This should be reflected with variations on the fitting parameters. But it is not possible to refine all the parameters together because they can be highly correlated. The final fit thus results from imposing initial restrictions on the set of fitting variables in order to attain a convergence with reasonable parameter values. The main advantage of this method is the possibility of obtaining physical information directly from the fitting parameters. The main disadvantage is that the fitting procedure requires deep knowledge of the experimental parameters (such as energy resolution), good theoretical description and fitting strategy.

4.2. Statistical parameters method

If spectra are considered as discrete probability distributions, some statistical parameters may be calculated to characterize them. The ones studied in this work are the area A_Z, the first moment FM_Z and the IAD_Z value [22]. These parameters are calculated in several spectral regions using the following relations:

$$A_Z = \sum_{i=i_{Zi}}^{i_{Zf}} I_i(E_{i+1}-E_i) \tag{1}$$

$$FM_Z = \frac{\sum_{i=i_{Zi}}^{i_{Zf}} E_i I_i(E_{i+1}-E_i)}{A_Z} \tag{2}$$

$$IAD_Z = \sum_{i=i_{Zi}}^{i_{Zf}} \left| I_i - I_i^{ref} \right| (E_{i+1}-E_i) \tag{3}$$

where I_i is the intensity of the spectrum for the channel i whose energy is E_i, Z is the region in which the parameters are calculated (defined by the channels i_{Zi} and i_{Zf}), and I_i^{ref} is the intensity for the channel i of a certain spectrum taken as reference. These parameters are very easy to calculate and do not depend on a user-criteria, except for Z region selection.

4.3. Minimum squares method

In some cases the XES spectrum can be considered as a linear combination of the spectra emitted by each of the compounds contained in the sample. This assumption requires no chemical interaction between the mixed compounds, so the electronic energy levels of the central atom considered in one compound do not affect the electronic levels in the others compounds and vice versa. Bearing this in mind, if I_i^k is the intensity at channel i corresponding to the k-pure non-mixed compound, the predicted intensity I_i^{pred} for the sample can be written as:

$$I_i^{pred} = \sum_{k=1}^{n} a_k I_i^k \tag{4}$$

where the coefficient a_k is the weight of the k-th spectrum and n is the total number of compounds in the sample. The best set of coefficients a_k can be obtained by minimizing the χ^2 function, which corresponds to the sum of the quadratic differences between the experimental and predicted intensities weighted by a factor. In this case, the weighting factor is the inverse of the square of the experimental error. The χ^2 function can be calculated as:

$$\chi^2 = \sum_{i=i_{Zi}}^{i=i_{Zf}} \frac{\left(I_i - I_i^{pred}\right)^2}{I_i} \tag{5}$$

The coefficients a_k represent the molecular concentration of each compound composing the sample. Some restrictions to the $\{a_k\}$ set (normalization conditions, positive or null values, etc.) may be included in the minimization procedure. If the measurements are not performed with the same incident flux, the method can still be applied to the spectra pre-normalized. The correlation matrix of the refined parameters, or the result of the minimization without the normalization condition, can be used to estimate the uncertainty of the method.

4.4. Principal component analysis

The principal component analysis is one of the many multivariate analysis techniques available and can be helpful when trying to understand the existing variability in a set of multivariate data, like in a set of spectra, in which each channel can be considered as a variable [23]. If p variables (intensity corresponding to each energy channel of a spectrum) are measured for n samples, then an $n \times p$ matrix, called X matrix, can be constructed. The basic idea of PCA is to get an expression for the axes of a new coordinate system that is centered on the data cloud, and rotated to be aligned its axes of maximum variance. These new axes are called the Principal Components, and the axis that is aligned with the maximum variance axis is called Principal Component 1 (PC1); the following is the Principal Component 2 (PC2), and so on. Each of these PCs is a specific linear combination of the original variables, orthogonal to each other, so the variability of the dataset explained by on one of them is not contained in the others. The values of these PCs, resulting of specific linear combinations, were called PCs scores. The PCA method allows the user to explore the total variability in smaller "fractions", by looking at the projections of the dataset into different principal component bi-dimensional planes [24].

5. Results and discussion

5.1. Mn oxides mixtures

The high-resolution Kβ emission spectra measured for the Mn oxides mixtures are shown in Fig. 2. Spectra were normalized to the area of the Kβ′ – $K\beta_{1,3}$ region, which is chemically invariant [2], in order to avoid possible influences due to matrix effects and fluctuations of the incident flux of X-rays. The most relevant parameters for Mn speciation in each methodology are presented in the following sections. Table 1 summarizes the results obtained and includes an estimation of the uncertainty of the molecular MnO concentration.

5.1.1. Fundamental parameters method

For the fitting, the energy position of $K\beta_x$ and RAE were fixed to 1.82 eV and 2.54 eV to the left of the energy position of the main $K\beta_{1,3}$ line, respectively, which was refined for each spectrum. The asymmetry parameter of the RAE function was constrained between −6.2 and −6.7. The same Gaussian/Lorentzian widths for $K\beta_x$ and $K\beta_{1,3}$ were used. In case of RAE structure, the parameters fitted were: area, width, and asymmetry of EMG function. The energy, width, and area of Kβ′ structure were fitted. For $K\beta_x$ the area was refined and for $K\beta_{1,3}$ area, energy position, Gaussian, and Lorentzian widths were optimized. To study the spectral features in the high energy region, the contribution of the tail of the main $K\beta_{1,3}$ line was removed by using a Lorentzian

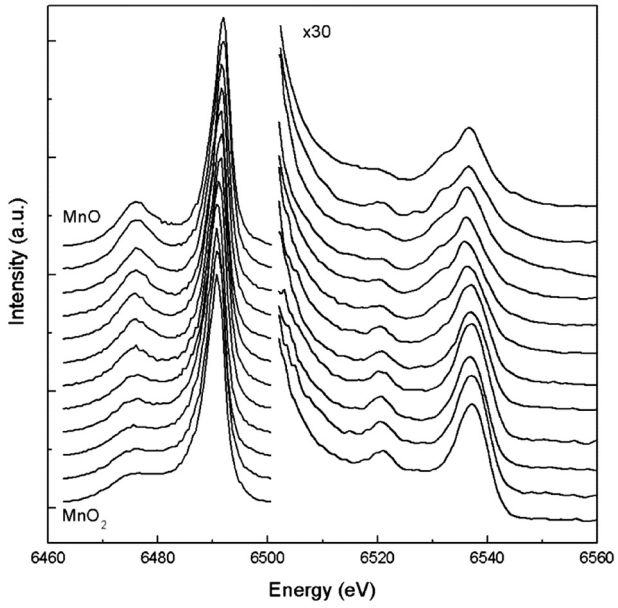

Fig. 2. High resolution Kβ emission spectra for the Mn oxide mixtures studied in this work. From top to bottom: the spectra are ordered as samples description in Section 3.1. The Kβ″–$Kβ_5$ region was expanded in order to make clear its structure.

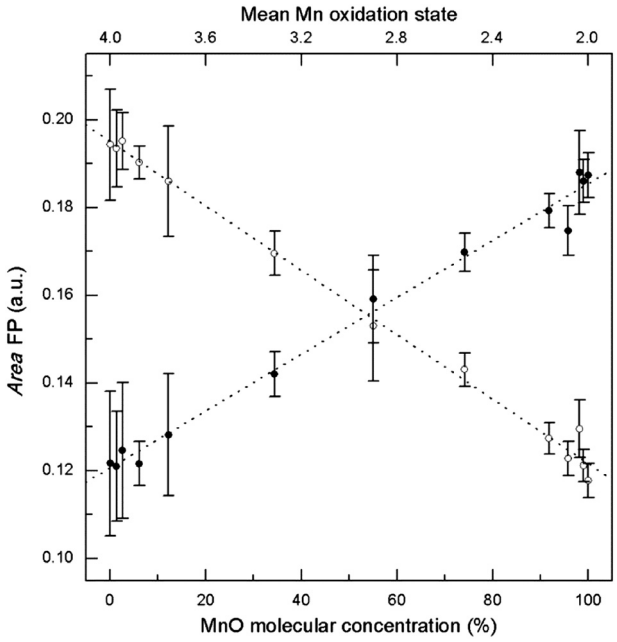

Fig. 3. Areas obtained for Kβ′ (●) and RAE (○) lines by fundamental parameter fitting procedure for mixtures of Mn^{2+} and Mn^{4+} oxides as a function of the molecular concentration of MnO. The dotted lines correspond to the linear fits. The error bars were determined by error propagation of fitting process.

function which was fitted to several data points of the $Kβ_{1,3}$ tail above and below the spectral features in this region [21]. Then, Kβ″ structure was fitted with one Voigt function for spectra corresponding to samples with MnO concentration lower than 30%, and with two Voigt functions sharing both Gaussian and Lorentzian widths for the other spectra. The $Kβ_5$ structure was properly described by two/three Voigt functions for samples with MnO concentration lower/higher than 30%, respectively. All the functions used for Kβ″ and of $Kβ_5$ structures had the same Lorentzian widths.

The parameters that present a clear linear behavior are the Kβ′, RAE and Kβ″ areas, and the energy difference between the $Kβ_5$ structure and the $Kβ_{1,3}$ line) (Figs. 3 and 4), which are in agreement with results obtained by others authors [2–5]. The error bars in Figs. 3 and 4 corresponds to the uncertainties associated to the fitting process. Some of the other parameters fitted present a weaker tendency with the oxidation state. For instance, Kβ′ and RAE widths decrease when the MnO molecular concentration increases and the energy difference between $Kβ_{1,3}$ and Kβ′ peaks slightly increases, going from 15.6 eV for low MnO concentration up to 16 eV for the higher MnO concentrations.

Table 1
The coefficient of determination R^2 and the E_{MnO}: uncertainty estimation for Mn^{2+} concentration determination in sample $MnO_{0.50}$, for the statistical parameters used.

	Parameter	R^2	E_{MnO}
Fundamental parameters	A_z for Kβ′ region	0.9846	10%
	A_z for RAE region	0.9936	9%
	E $Kβ_5$ − E $Kβ_{1,3}$	0.9694	12%
	A_z for Kβ″ region	0.9721	10%
Statistical	A_z for Kβ′ region	0.9878	5%
	IAD_z for Kβ′ region	0.9745	10%
	IAD_z for $Kβ_{1,3}$ + Kβ' region	0.9643	13%
	FM_z for Kβ″ region	0.9932	8%
	FM_z for $Kβ_5$ region	0.9285	15%
	A_z for Kβ″ region	0.9345	12%
	IAD_z for $Kβ_5$ region	0.9567	15%
Mean square	a_1 for Kβ′ region	0.9950	4.5%
	a_1 for Kβ″ - $Kβ_5$ region	0.9966	4.5%
PCA	PC1 for Kβ′ - $Kβ_{1,3}$ region	0.9586	9%
	PC1 for Kβ″ - $Kβ_5$ region	0.9638	9%

From the parameters studied, it was possible to calculate the energy difference between the $Kβ_5$ structure and the Kβ″ line, which resulted almost constant: (15.7 ± 0.4) eV. This value agrees very well with the theoretical value of ~16 eV, corresponding to the energy difference between the ligand 2 *s* and 2*p* energy levels [25].

Despite the difficulty inherent to this method which involves a deconvolution procedure with constraints, it allows obtaining

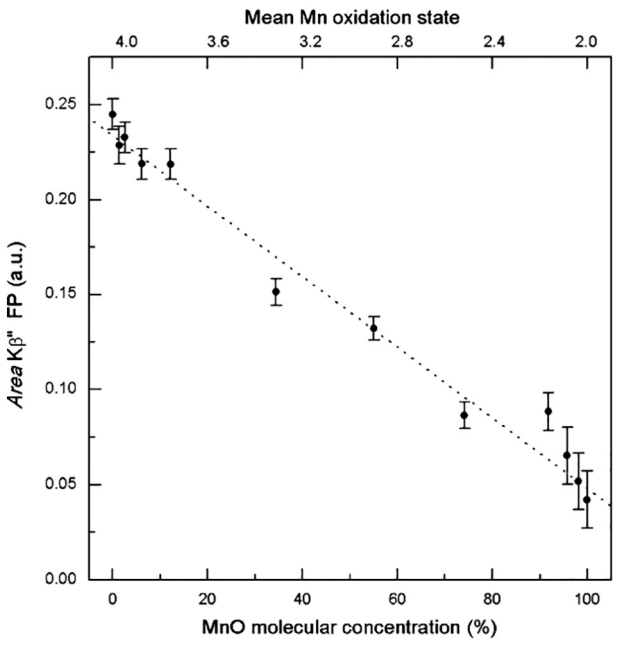

Fig. 4. Area obtained for Kβ″ line (●) by fundamental parameter fitting procedure for mixtures of Mn^{2+} and Mn^{4+} oxides as a function of the molecular concentration of MnO. The dotted lines correspond to the linear fits. The error bars were determined by error propagation of fitting process.

additional data not covered by the other methods presented such as natural linewidths, or peak asymmetry parameters.

5.1.2. Statistical parameters method

For the *IAD* calculation, the spectrum of MnO oxide was used as the reference and spectra were aligned on the $K\beta_{1,3}$ peak in order to avoid spurious contributions to the parameters due slights variations in energy calibration [22].The uncertainties associated with each determination were estimated by propagating the errors of the intensity values through the Eqs. (1)–(3). Fig. 5 shows the behavior of the IAD_z as a function of the MnO molecular concentration, calculated in the *Z* regions corresponding to the Kβ′: [6462.7–6481.8] eV and Kβ′ + $K\beta_{1,3}$: [6462.7–6504.3] eV structures. Both parameters present a linear correlation, although the IAD_z in Kβ′ – $K\beta_{1,3}$ region has a greater dispersion, it presents a greater relative variation. The A_z parameter calculated in Kβ′ region presents the same behavior than IAD_z, although the error associated with each determination and the regression coefficient for the linear fit is slightly better (see Table 1). The FM_Z determined in the area corresponding to Kβ″ [6510.8–6524.2] eV and $K\beta_5$ [6524.8–6550.7] eV decreases linearly with the MnO concentration, with a variation of about 0.4 eV for a change from +4 to +2 in the oxidation state (Fig. 6). The average difference between the $FM_{K\beta''}$ and $FM_{K\beta5}$ is (17.45 ± 0.07) eV and practically does not vary with the oxidation state. This latter value is slightly higher than the theoretical value expected ~16 eV [25], given that *FM* underestimates the peak energies due to the influence of $K\beta_{1,3}$ tail. Fazinic et al. [26] shows that the experimental values of difference energies of Kβ″ and Kβ5 lines of several authors and techniques are in a range of approximately [13.6–18.8] eV, with an average value of 15.3 eV.

Fig. 7 shows the behavior of A_z calculated in the Kβ″ region [6524.8–6550.7] eV, which decreases with the MnO molecular concentration. This is expected since the intensity of this line is strongly related to the number of first O neighbors (8 in these spectra) and the Mn–O distance (2.2230 Å for MnO and 1.8797 Å for MnO_2) [25].

Both the A_z parameter and the IAD_z have an increasing behavior with the MnO mass concentration and the final error associated is similar (see Table 1). The Kβ″ – $K\beta_5$ region has approximately an intensity ratio of 1:30 ratio with respect to $K\beta_{1,3}$ region for Mn oxides (see Fig. 1), which implies an important contribution in the error due to the statistical counting, resulting in a greater error in the quantification of MnO. All the statistical parameters studied exhibited a clear linear behavior with the MnO concentration. As it was mentioned above, the Kβ″ and $K\beta_5$ structures lie in high energy tail of the main $K\beta_{1,3}$ line. On possibility to minimize the influence of the main peak is to remove the background [21] (see Fig. 1). This background removal involves a fitting

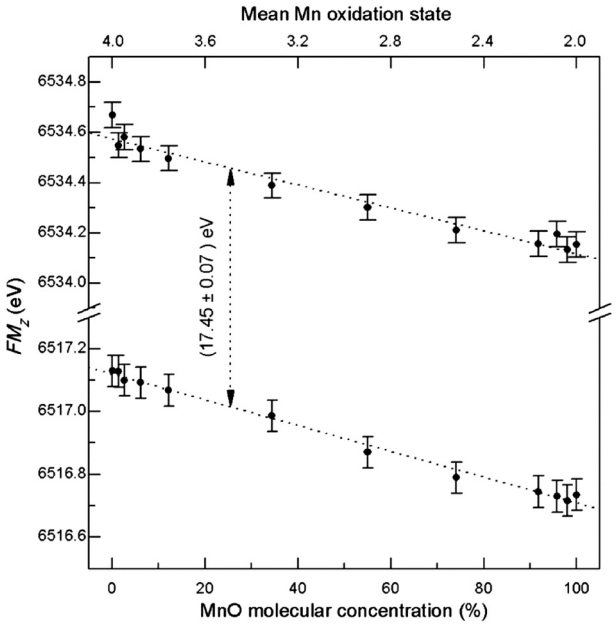

Fig. 6. First moment of the Kβ″ (bottom) and $K\beta_5$ (top) region for mixtures of Mn^{2+} and Mn^{4+} oxides as a function of the molecular concentration of MnO. The dotted line corresponds to the linear fit. The error bars were obtained by propagating the errors of the intensity values through the Eq. (2).

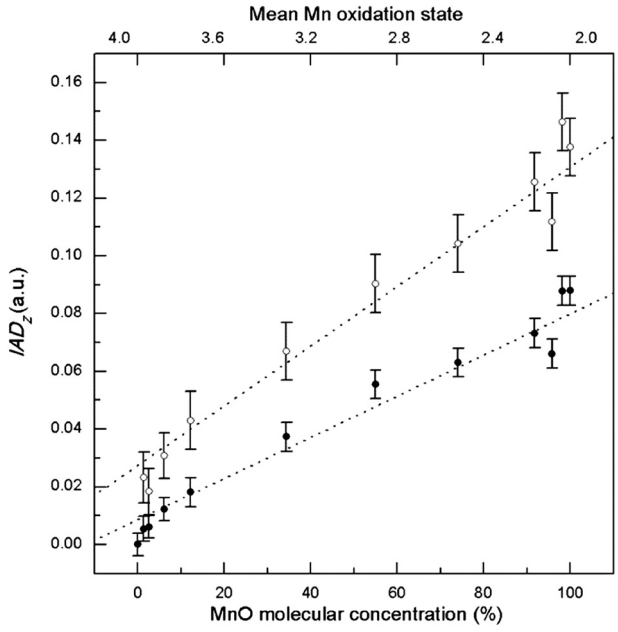

Fig. 5. Statistical parameters IAD_z, calculated in the Kβ′ (●) and Kβ′ + $K\beta_{1,3}$ (○) regions for mixtures of Mn^{2+} and Mn^{4+} oxides as a function of the molecular concentration of MnO. The dotted lines correspond to the linear fits. The error bars were obtained by propagating the errors of the intensity values through the Eq. (3).

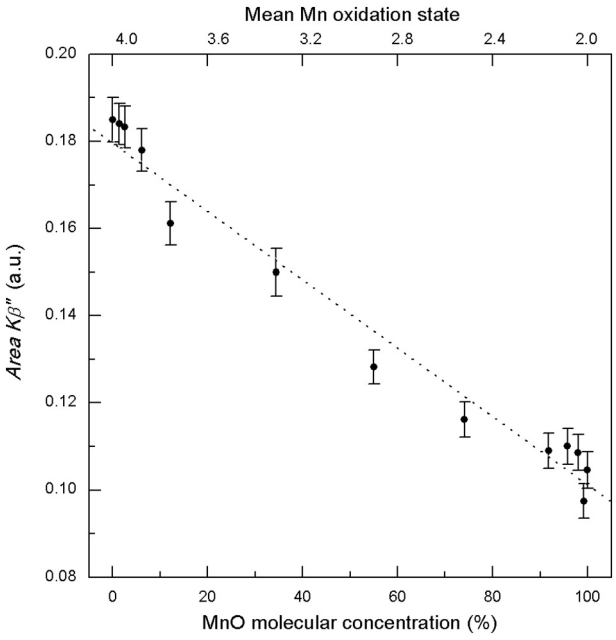

Fig. 7. Statistical parameters A_z, calculated in the Kβ″ region for mixtures of Mn^{2+} and Mn^{4+} oxides as a function of the molecular concentration of MnO. The dotted lines correspond to the linear fits. Error bars were obtained by propagating the errors of the intensity values through the Eq. (1).

procedure, which turns the approach into a mixture of statistical and FP approaches. However, this approach can be very useful when precise values of areas and energies are required, for example to compare with theoretical results.

5.1.3. Minimum squares method

In this method, the measured spectrum I is considered as a linear combination of the spectra emitted by each pure oxide: $I = a_1 I_1 + a_2 I_2$, where subscript *1* and *2* referred to MnO and MnO_2, respectively. It is important to highlight that the χ^2 function (see eq. 5) gives more weight to the channels with greater intensity. In this sense, if the $K\beta_{1,3}$ region where completely included, the contribution of Kβ′ would be reduced, which is the one that has sensitivity to the oxidation state. An alternative to take into account the complete region would be using in the χ^2 function a weighting factor favoring the regions of lower intensity. Nevertheless, it was preferred to use the conventional definition of χ^2 function in a region of similar intensities including the Kβ′ line. An example of the minimum square fit is shown in Fig. 8 for the $MnO_{0.30}$, a Mn oxide mixture sample. The coefficients a_k, determined for Kβ′ region (see Fig. 1), are presented in Fig. 9. The only constraint imposed in the minimization was $a_k \geq 0$. The deviation of $a_1 + a_2$ from unity was used to estimate the uncertainties for each data. It can be seen from Fig. 9 that the parameter a_1 shows less dispersion than the a_2. In the case of the coefficient a_1, the deviations from the nominal value are lower than 3% in all cases, except for the spectrum corresponding to 0.741% of MnO, where the dispersion reached 10%. The coefficients a_k, determined for Kβ″ – $K\beta_5$ region by the same procedure described previously, were also calculated. In general, the errors are considerably smaller than the ones obtained for the Kβ′ region. This is because, despite the lower counting statistics, the overall variation of the spectra is more pronounced in the Kβ″ – $K\beta_5$ region. In addition, the minimum squares method requires a large zone in the spectra, with similar intensity values in order to weight similarly each channel.

5.1.4. Principal component analysis

Two regions were identified from a first PCA of the entire spectrum as the regions of interest: Kβ′ – $K\beta_{1,3}$ and Kβ″ – $K\beta_5$ structures (see Fig. 1). Then, a second PCA analysis was performed to obtain a projection of the measured spectra in the PC1 – PC2 plane, from which it was found

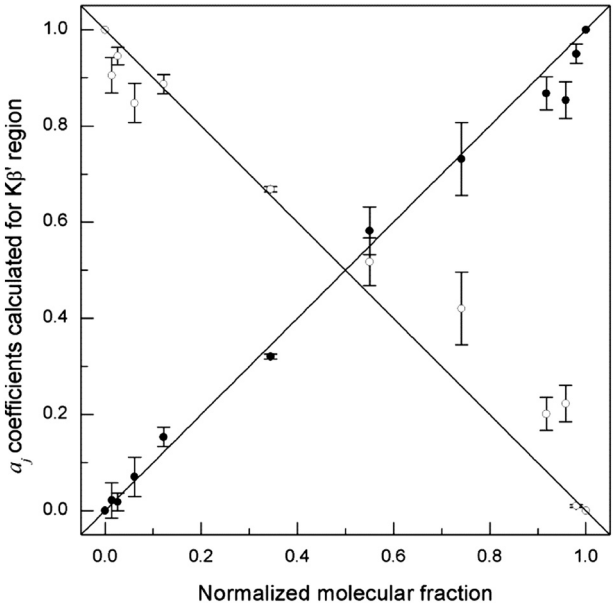

Fig. 9. Coefficients resulting from the minimum squares minimization for the mixture of Mn oxides in the Kβ′ region: a_1 (●) and a_2 (○) referred to MnO and MnO_2, respectively. The solid lines correspond to the nominal values of each parameter. Error bars were estimated as the deviation of $a_1 + a_2$ from unity.

that PC1 represents the 98.4% of the total variability, and the data dispersion does not allow discriminating MnO concentrations below 5% or above 95%. Fig. 10 shows the relation between MnO molecular concentration and the PC1 scores obtained from the PCA in the Kβ″ – $K\beta_5$ region. A linear tendency with slight data dispersion can be observed, showing that PC1 is a sensitive variable of the Mn chemical environment, which can be useful as a parameter for the desired quantification. A similar behavior was obtained when PC1 scores for Kβ′ – $K\beta_{1,3}$ region is considered as function of MnO molecular concentration.

The regression values for the linear fits of the studied parameters are shown in Table 1. By performing error propagation through the linear coefficients and considering the statistical errors, an estimation of the

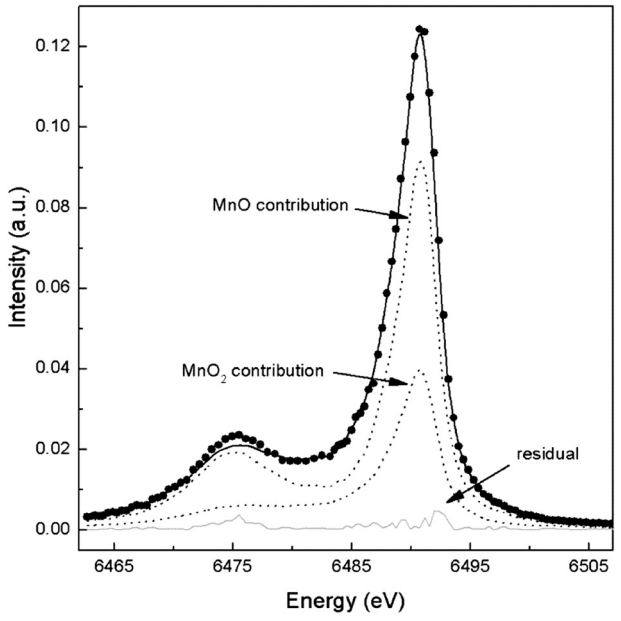

Fig. 8. High-resolution Kβ spectrum of $MnO_{0.30}$ sample (●) fitted by a linear combination of MnO and MnO_2 spectrum contribution, using the *Minimum square method*. The residual of fitting process is also shown.

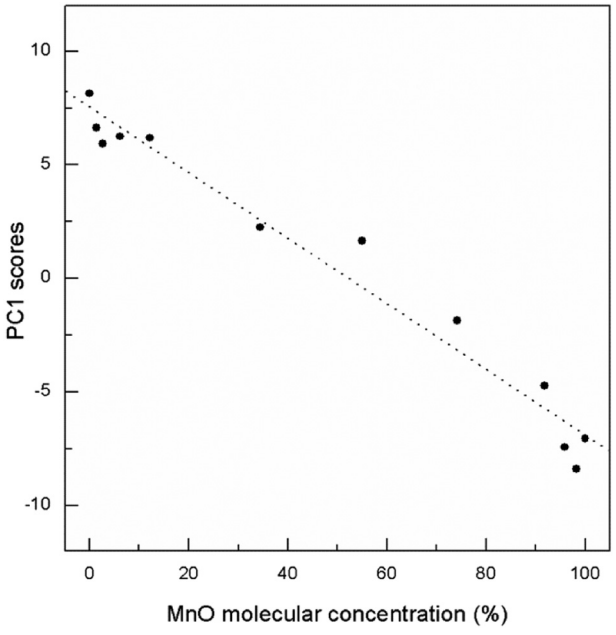

Fig. 10. PC1 scores calculated in the Kβ″ – $K\beta_5$ region as a function of MnO molecular concentration in the mixtures of Mn^{2+} and Mn^{4+}compound. The dotted line corresponds to the linear fit.

uncertainty (E_{MnO}) related to the determination of Mn^{2+} concentration in a sample with 50% MnO is included. For the minimum squares method, the E_{MnO} error corresponds to the maximum value between the error of parameter a_1 and the difference between the values of a_1 and the nominal concentration. The regression values for the linear fits of the PC1 scores in both regions are also shown in Table 1.

5.2. Perovskites

The effective existence of Mn^{2+}/Mn^{3+} mixed valence in these DPOs has been previously probed by XES measurements using the fundamental parameters method [7], but a rigorous study of the uncertainties related to the method used was not presented. A correct normalization of the spectra is very important here since the unknown samples have a very different matrix respect to the reference spectra used. Therefore each spectrum was normalized to the total integrated intensity in the Kβ region. The spectra measured for the DPOs are shown in Fig. 11. Region of the spectrum corresponding to Kβ″ and $K\beta_5$ structures were not measured for the DPOs samples because of it very low counting rate. The samples taken as reference are the pure oxides MnO, Mn_2O_3, and MnO_2. For the minimum squares method, only MnO and Mn_2O_3 spectra were used since no Mn^{4+} presence is expected in the samples analyzed.

The implementation of the fundamental parameter method was similar to that used for fitting the Mn oxides mixtures. As a result, the Kβ′ and RAE areas show linear tendencies with the nominal Mn oxidation state, in agreement to a previous work [7], but the estimated oxidation state from the linear fit are not exactly the same, caused by different fitting strategies. According to previous works [7], a region strongly influenced by the oxidation state is the RAE structure. This contribution, together with the $K\beta_x$ line, is responsible for the low energy asymmetry present in the main Mn-$K\beta_{1,3}$ line (Fig. 1). A statistical parameter that reflects the behavior of this asymmetry is the area A_{RAE} (Fig. 12), calculated according to Eq. (1) in the region corresponding to the asymmetric zone. The statistical A_{RAE} data increases with the oxidation state, like the corresponding area obtained by the fundamental parameters method, but the points lie slightly below the calibration curve (dotted line in Fig. 12). This is because the statistical A_{RAE} parameter includes a contribution of the $K\beta_x$ line. Two effects compete in the same region: while the A_{RAE} increases with the oxidation state, the area of the $K\beta_x$ line decreases, so the statistical A_{RAE} area underestimates the real one.

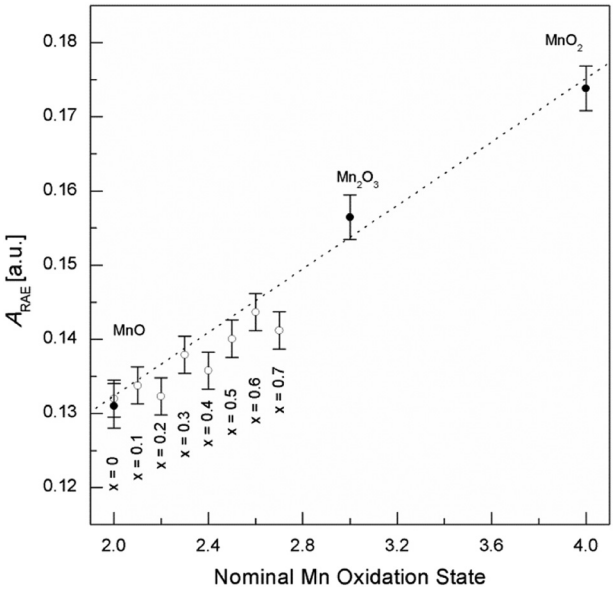

Fig. 12. Statistical parameter A_z calculated in the RAE region, as shown in Fig. 1, as a function of the nominal Mn oxidation state for double perovskite oxides $Ba_{1+x}La_{1-x}MnSbO_6$ ($0 \le x \le 0.7$) (○) and for the reference Mn pure oxides (●).The dotted line corresponds to the linear fit of reference data. Error bars were obtained by propagating the errors of the intensity values through the Eq. (1).

Minimum squares method was applied in the Kβ′ region using as reference spectra the corresponding to pure oxides MnO and Mn_2O_3, and imposing the normalization condition to a_k coefficients. In this case, the region considered was restricted only to the Kβ′ line, since this region showed greater sensitivity to the chemical environment of Mn than the $K\beta_{1,3}$ line, considering that the samples have very similar mean oxidation states. Besides, the higher intensity of $K\beta_{1,3}$ with respect to Kβ′ will give it a higher importance in the $\chi 2$ calculation procedure. The oxidation state was then calculated by using the a_k coefficients (calculated oxidation state $= 2a_{MnO} + 3a_{Mn2O3}$). As can be seen in Fig. 13,

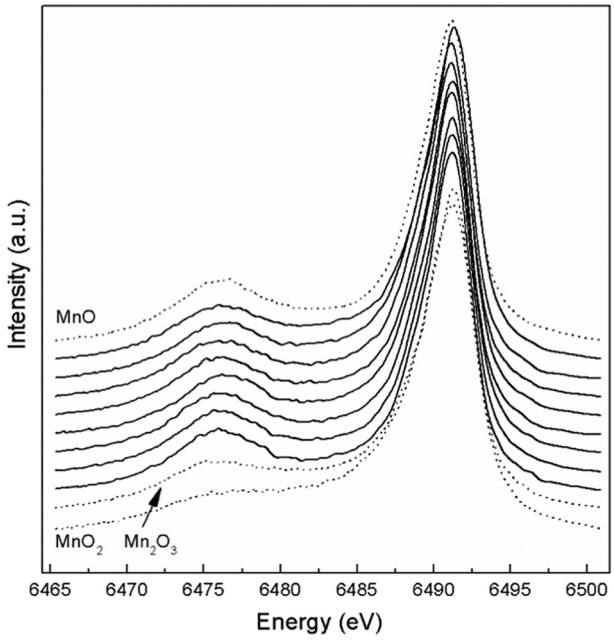

Fig. 11. High resolution Kβ emission spectra for the MnO, Mn_2O_3 and MnO_2 oxides and the DPOs $Ba_{1+x}La_{1-x}MnSbO_6$, with x = 0, 0.1, 0.2, 0.3, 0.4, 0.5, 0.6, and 0.7, from bottom to top, respectively.

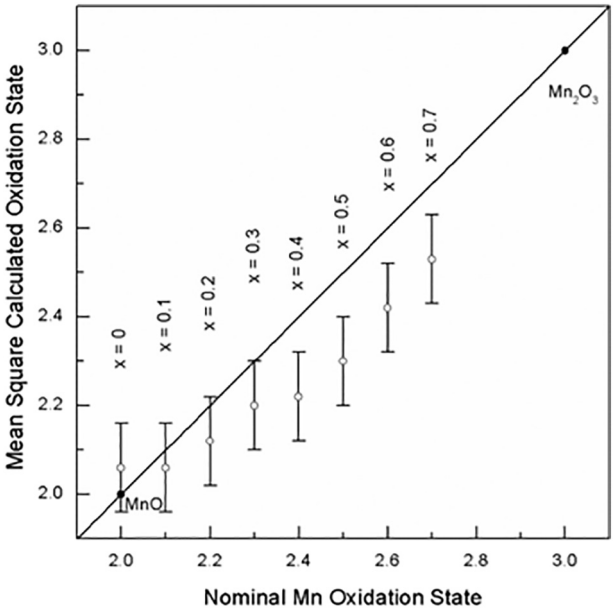

Fig. 13. The calculated oxidation state by minimum square method for double perovskite oxides $Ba_{1+x}La_{1-x}MnSbO_6$ ($0 \le x \le 0.7$) (○) and for the reference Mn pure oxides (●). The solid line corresponds to the nominal values of oxidation state. The error bars corresponds to the error of 5%, estimated for the analysis of oxide mixtures (see Table 1).

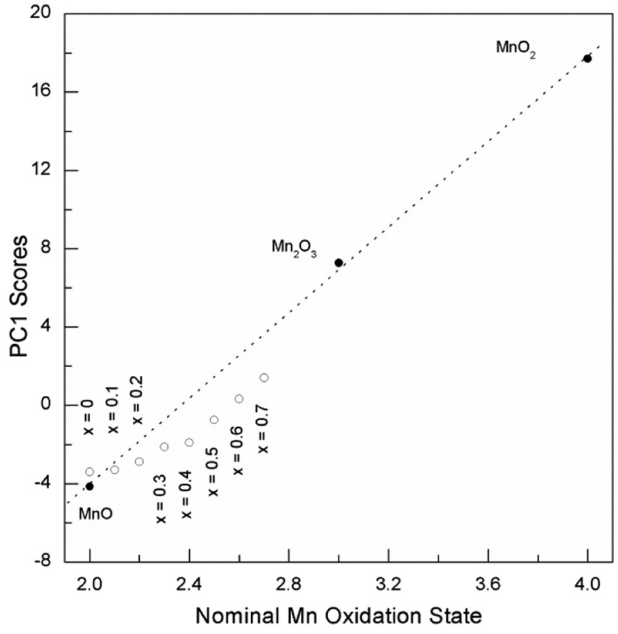

Fig. 14. PC1 scores calculated, considering the Kβ′ – RAE region as a function of nominal Mn oxidation state for double perovskite oxides $Ba_{1+x}La_{1-x}MnSbO_6$ ($0 \le x \le 0.7$) (○) and for the reference Mn pure oxides (●). The dotted line corresponds to the linear fit of reference data.

the calculated oxidation state increases with the x value and are below the values predicted by the nominal oxidation state for samples with x higher than 0.4.

By analyzing the PC1 loading of a PCA applied to the Kβ′ – $K\beta_{1,3}$ structures, the regions [6474.0–6478.0] eV and [6481.0–6485.4] eV were found more sensitive to the oxidation state. These sub-regions correspond to the Kβ′ and RAE structures (see Fig. 1). The obtained PC1 scores for the PCA performed in the sub-region mentioned are shown in Fig. 14, as a function of nominal Mn oxidation state.

Table 2 shows, comparatively, the calculated oxidation states and their estimated error for the double perovskites oxides by using the different analysis methods proposed. The oxidation states of DOPs samples were determined by the parameters of equation of the best-fit line, as shown in Figs. 12 and 13. The calculated DOPs uncertainties were determined by error propagation of fitting procedure. The values obtained by other authors are also presented. All the parameters studied show that the oxidation state of Mn increases with the value of x. However, statistical and multivariate methods show that the calculated Mn oxidation state is less than $+2(1 + x)$ (nominal Mn oxidation state) for $x > 0.2$ and this difference is greater as x increases. According to XRD results [7], the Mn-O distance is higher than the corresponding to Mn^{2+} oxide for $x = 0$, whereas it is lower than distance corresponding to Mn^{3+} oxide for $x > 0.4$. This deviation on the atomic distances may be responsible for a change in the charge distribution, and then in the resulting oxidation state.

6. Conclusions

Kβ HR-XES was applied to study and quantify the Mn oxidation state in different kind of samples. These spectra were measured using a non-conventional spectrometer with conventional X-ray sources making it a versatile and low-cost approach compared to HR-XES based on synchrotron radiation. Chemical information was obtained by the characterization of several spectral features of the measured spectra. Three different methodologies were tested for obtaining parameters useful to estimate the mean Mn oxidation state and its corresponding error. The methodologies were applied to two groups of samples: mixtures of Mn^{2+} and Mn^{4+} oxides and double perovskite oxides $Ba_{1+x}La_{1-x}MnSbO_6$ (with $0 \le x \le 0.7$). The applied methodological techniques proved their usefulness in the analysis of this type of spectra and the characterization of the Mn chemical environment.

The fundamental parameter method requires a complete theoretical description of the X-ray spectrum and the final parameters optimized depend strongly on the constraints and fitting criteria used. However, it is well-known that this method provides valuable information regarding the chemical environment of a 3*d* transition metal as well as the electronic structure. The statistical parameters and the minimum square method are simple to calculate and do not depend on the user criteria, except for the selection of the spectral region where the parameters are calculated. PCA has extensively demonstrated its ability to highlight and characterize the variability in a set of spectra. The last two approaches are recommended for extracting information about the oxidation state in a fast way.

The statistical and fundamental parameters calculated in $K\beta_5$ region are highly affected by the statistical counting error. Nevertheless, this region presents the largest relative variation and it is worth considering as an additional probe of the oxidation state. One possibility to minimize the influence of the main $K\beta_{1,3}$ line over $K\beta_5$ region is to remove the background by a appropriated fitting procedure [21], which converts the approach into a mixture of statistical and FP approaches. This approach can be very useful when precise values of areas and energies are required, for example to compare with theoretical results. Whether using the main region of the high-resolution spectrum (Kβ′ – $K\beta_{1,3}$ region) or the high-energy region (corresponding to Kβ″ and $K\beta_5$ structures) is possible to quantify the Mn oxidation states. From the linear fit of reference samples data, the mean Mn oxidation state can be determined with an error between 0.1 and 0.2, which corresponds to a relative error between 4% and 10% for the double perovskite oxides studied. It was found that the calculated oxidation states of Mn, using statistical

Table 2
Calculated Mn oxidation state from the proposed analysis methods for double perovskite oxides $Ba_{1+x}La_{1-x}MnSbO_6$ ($0 \le x \le 0.7$). The uncertainties are shown between parentheses[a].

Calculated Mn oxidation state						
Sample	Fundamental parameters		Statistical	Min. Square	PCA	Ref. 6
	$A_{K\beta'}$	A_{RAE}	A_{RAE}	a_1	PC1	$A_{K\beta'}$
x = 0	2.35 (0.20)	2.15 (0.20)	1.98 (0.20)	2.06 (0.10)	2.05 (0.10)	2.0 (0.1)
x = 0.1	2.20 (0.20)	2.17 (0.20)	2.06 (0.20)	2.06 (0.10)	2.06 (0.10)	2.2 (0.1)
x = 0.2	2.26 (0.20)	2.14 (0.20)	2.00 (0.20)	2.15 (0.10)	2.10 (0.10)	2.2 (0.1)
x = 0.3	2.31 (0.20)	2.35 (0.20)	2.26 (0.20)	2.20 (0.10)	2.17 (0.10)	2.3 (0.1)
x = 0.4	2.38 (0.20)	2.43 (0.20)	2.16 (0.20)	2.22 (0.10)	2.19 (0.10)	2.4 (0.1)
x = 0.5	2.66 (0.20)	2.69 (0.20)	2.36 (0.20)	2.30 (0.10)	2.30 (0.10)	2.5 (0.1)
x = 0.6	2.54 (0.20)	2.82 (0.20)	2.53 (0.20)	2.42 (0.10)	2.39 (0.10)	2.6 (0.1)
x = 0.7	2.64 (0.20)	2.82 (0.20)	2.41 (0.20)	2.53 (0.10)	2.49 (0.10)	2.7 (0.1)

[a] The calculated DOPs uncertainties were determined by error propagation on the linear fits, except for the minimum square method for which a value of 5% was used, estimated by the analysis of oxide mixtures.

parameters and PCA analysis, show an increasing tendency lower than that of simple Mn oxides used as standards. This behavior must be related to the global changes (structural and electrical/magnetic properties) of the DOPs samples [7], which are much more complex than the Mn oxides. Despite the errors of the calculated oxidation states, the obtained parameters allow to see a clear increase with the variable *x*.

Acknowledgments

Financial support from the Consejo Nacional de Investigaciones Científicas y Técnicas (CONICET) (PICT-2016-0285). The authors gratefully acknowledge to Prof. R. Carbonio and their colleagues to access to use their DPOs samples.

References

[1] S. Vasala, M. Karppinen, $A_2B'B''O_6$ perovskites: a review, Prog. Solid State Chem. 43 (2015) 1–36.
[2] P. Glatzel, U. Bergmann, High resolution 1s core hole X-ray spectroscopy in 3d transition metal complexes-electronic and structural information, Coord. Chem. Rev. 249 (2005) 65–95.
[3] S. Limandri, S. Ceppi, G. Tirao, G. Stutz, C.G. Sánchez, J.A. Riveros, High resolution study of Kβ′ and $K\beta_{1,3}$ X-ray emission lines from Mn-compounds, Chem. Phys. 367 (2010) 93–98.
[4] U. Bergmann, P. Glatzel, X-ray emission spectroscopy, Photosynth. Res. 102 (2009) 255–266.
[5] S. Ceppi, A. Mesquita, F. Pomiro, E.V. Pannunzio Miner, G. Tirao, Study of Kβ X-ray emission spectroscopy applied to Mn(2-x)V(1 + x)O4 (x = 0 and 1/3) oxyspinel and comparison with XANES, J. Phys. Chem. Solids 75 (2014) 366–373.
[6] M. Petric, R. Bohinc, K. Bučar, M. Žitnik, J. Szlachetko, M. Kavčič, Chemical state analysis of phosphorus performed by X-ray emission spectroscopy, Anal. Chem. 87 (2015) 5632–5639.
[7] D.M. Arciniegas Jaimes, M.C. Blanco, F. Pomiro, G. Tirao, V.M. Nassif, G. Cuello, J.A. Alonso, R.E. Carbonio, Synthesis, structural characterization and magnetic properties of the series of double perovskites $Ba_{1+x}La_{1-x}MnSbO_6$ with 0.1 ≤ x ≤ 0.7, J. Alloys Compd. 704 (2017) 776–787.
[8] M.A. Beckwith, M. Roemelt, M. Collomb, C. DuBoc, T. Weng, U. Bergmann, P. Glatzel, F. Neese, S. DeBeer, Manganese Kβ X-ray emission spectroscopy as a probe of metal–ligand interactions, Inorg. Chem. 50 (2011) 8397–8409.
[9] E. Gallo, F. Bonino, J.C. Swarbrick, T. Petrenko, A. Piovano, S. Bordiga, D. Gianolio, E. Groppo, F. Neese, C. Lamberti, P. Glatzel, Preference towards five-coordination in Ti silicalite-1 upon molecular adsorption, ChemPhysChem. 14 (2013) 79–83.
[10] K.M. Lancaster, K.D. Finkelstein, S. DeBeer, Kβ X-ray emission spectroscopy offers unique chemical bonding insights: revisiting the electronic structure of ferrocene, Inorg. Chem. 50 (2011) 6767–6774.
[11] G. Peng, F.M.F. de Groot, K. Hämäläinen, J.A. Moore, X. Wang, M.M. Grush, J.B. Hastings, D.P. Siddons, W.H. Armstrong, O.C. Mullins, S.P. Cramer, High-resolution manganese X-ray fluorescence spectroscopy. Oxidation-state and spin-state sensitivity, J. Am. Chem. Soc. 116 (1994) 2914–2920.
[12] E. Cengiz, Z. Bıyıklıoğlu, N. Küp Aylıkcı, V. Aylıkcı, G. Apaydın, E. Tıraşoğlu, H. Kantekin, Chemical effect on K shell X-ray fluorescence parameters and radiative auger ratios of Co, Ni, Cu, and Zn complexes, Chin. J. Chem. Phys. 23 (2010) 138–144.
[13] D. Mitra, M. Sarkar, D. Bhattacharya, L. Natarajan, Satellites, hypersatellites and RAE from Ti, V, Cr, Mn and Fe in photoionization, X-Ray Spectrom. 37 (2008) 585–594.
[14] S.P. Limandri, A.C. Carreras, R.D. Bonetto, J.C. Trincavelli, Kβ satellite and forbidden transitions in elements with 12 ≤ Z ≤ 30 induced by electron impact, Phys. Rev. A: At. Mol. Opt. Phys. 81 (2010), 012504. (10 p).
[15] H. Adachi, S. Shiokawa, M. Tsukada, C. Satoko, S. Sugano, Discrete variational Xα cluster calculations. III. Application to transition metal complexes, J. Phys. Soc. Jpn. 47 (1979) 1528–1537.
[16] G. Tirao, S. Ceppi, A.L. Cappelletti, E.V. Pannunzio Miner, Oxidation state characterization in Cr oxides by means of Cr-Kβ emission spectroscopy, J. Phys. Chem. Solids 71 (2010) 199–205.
[17] M. Torres Deluigi, F.M.F. de Groot, G. López-Díaz, G. Tirao, G. Stutz, J. Riveros de la Vega, Core and valence structures in Kβ X-ray emission spectra of chromium materials, J. Phys. Chem. C 118 (2014) 22202–22210.
[18] Q. Zhou, B.J. Kennedy, C.J. Howard, M.M. Elcombe, A.J. Studer, Structural phase transitions in $A_{2-x}Sr_xNiWO_6$ (A = Ca or Ba, 0 ≤ x ≤ 2) double perovskites, Chem. Mater. 17 (2005) 5357–5365.
[19] M.C. Blanco, J.M.D. Paoli, S. Ceppi, G. Tirao, V.M. Nassif, J. Guimpel, R.E. Carbonio, Synthesis, structural characterization and magnetic properties of the monoclinic ordered double perovskites $BaLaMSbO_6$, with M = Mn, Co and Ni, J. Alloys Compd. 606 (2014) 139–148.
[20] G. Tirao, G. Stutz, C. Cusatis, An inelastic X-ray scattering spectrometer at LNLS, J. Synchrotron Radiat. 11 (2004) 335–342.
[21] E. Gallo, P. Glatzel, Valence to core X-ray emission spectroscopy, Adv. Mater. 26 (2014) 7730–7746.
[22] G. Vankó, T. Neisius, G. Molnár, F. Renz, S. Kárpáti, A. Shukla, F.M.F. de Groot, Probing the 3d spin momentum with X-ray emission spectroscopy: the case of molecular-spin transitions, J. Phys. Chem. B 110 (2006) 11647–11653.
[23] R.A. Johnson, D.W. Wichern, Applied Multivariate Statistical Analysis, Prentice Hall, Inc., Upper Saddle River, NJ, 1992.
[24] J. Robledo, H.J. Sánchez, J.J. Leani, C.A. Pérez, Exploratory methodology for retrieving oxidation state information from X-ray resonant Raman scattering spectrometry, Anal. Chem. 87 (2015) 3639–3645.
[25] U. Bergmann, C.R. Horne, T.J. Collins, J.M. Workman, S.P. Cramer, Chemical dependence of interatomic X-ray transition energies and intensities – a study of Mn Kβ′ and $K\beta_{2,5}$ spectra, Chem. Phys. Lett. 302 (1999) 119–124.
[26] S. Fazinić, L. Mandić, M. Kavčič, I. Božičević, Parametrization of Kβ″ and $K\beta_{2,5}$ X-ray contributions in Kβ spectra of 3d transition metal compounds, Anal. At. Spectrom. 26 (2011) 2467–2476.